Pergamon

PII: S0038–092X(02)00003–8

Solar Energy Vol. 72, No. 4, pp. 317–325, 2002

0038-092X/02/$ - see front matter

www.elsevier.com/locate/solener

EFFECT OF WIND ON FLOW DISTRIBUTION IN UNGLAZED TRANSPIRED-PLATE COLLECTORS

L. H. GUNNEWIEK*, K. G. T. HOLLANDS**,† and E. BRUNDRETT**

*Hatch Associates Ltd., 2800 Speakman Drive, Sheridan Science and Industrial Park, Mississauga, Ontario, Canada L5K 2R7

**Department of Mechanical Engineering, University Avenue, University of Waterloo, Waterloo, Ontario, Canada N2L 3G1

Received 19 April 2001; revised version accepted 16 November 2001

Communicated by BRIAN NORTON

Abstract—Unglazed transpired-plate solar air heaters have proven to be effective devices for heating air directly from ambient on a once through basis. They have found applications in ventilation-air preheating and in crop-drying. Large collectors are now routinely built that cover the sides of sizeable buildings, and the problem of designing the system so that the flow of the air through the collector face is reasonably uniform and so that there is no 'outflow' over part of the collector face has been seen as a challenging one. The flow distribution was analyzed in an earlier study using a computational fluid dynamics (CFD) model, but that study was limited to the case where there is no wind present. The present paper extends the earlier study to the case where there is wind. Various building orientations are examined, at a wind speed of 5 m/s. The wind was found to reinforce those factors that tend to produce outflow, and in light of this study, the recommended minimum suction velocity required to avoid outflow has been raised from about 0.0125 m/s to about 0.03 m/s, depending on the building shape. On the other hand, there are possible strategies that can be adopted to reduce the effect of wind, and these are discussed.

1. INTRODUCTION

Unglazed, transpired solar collectors (Hollick and Peter, 1990; Kutscher *et al*., 1991, 1993) have been the subject of a number of recent investigations (Gunnewiek *et al*., 1996; Dymond and Kutscher, 1997; Arulanandam *et al*., 1999; Van Decker *et al*., 2001). They are effective devices for applications where outside air is to be heated directly, such as in heating ventilation air for buildings and in crop drying. The outside air in question is drawn straight from ambient, through the whole surface of a transpired, dark-coloured plate (the absorber plate) which has been perforated with holes, typically with a porosity about 0.5%. Tests conducted on several installations indicate that the unglazed transpired collector (UTC) works very well with annual solar collection efficiencies reaching 72% (Carpenter and Kokko, 1991). More than 70 large systems each having collector areas between 500 and 10,000 m^2 have been installed and are successfully operating for fresh-air heating in Canada, the United States, Germany, and Japan and heating process air for crop drying in countries throughout the world.

These collectors have been installed to cover areas on the sides of buildings of the order of thousands of square metres, and the problem of designing the system so that the air is sucked uniformly (or nearly so) over such large areas has been a daunting one. Without careful design, this suction can actually reverse over part of the collector, producing a substantial drop in system performance. Clearly the designer needs an analytical tool — like a computer code — that will predict the degree of flow non-uniformity and the associated performance penalty. Dymond and Kutscher (1997) described such a computer code, one that uses a pipe network analog of the real plate hydrodynamics. This latter code certainly constitutes a useful tool, particularly since its modest demand for computer time makes it suitable in a design context. It is not, however, as realistic as a computational fluid dynamics (CFD) code, which is now the standard approach to analyzing complex flow problems in industry (see, for example, Ferziger and Peric, 1997). Consequently, Gunnewiek *et al.* (1996) developed a more rigorous CFD tool and applied it to modeling some real UTC situations. The approach Gunnewiek *et al.* adopted was to use the CFD

†Author to whom correspondence should be addressed. Tel.: +1-519-888-4053; fax: +1-519-888-6197; e-mail: kholland@mecheng1.uwaterloo.ca

code to model just the flow in the plenum behind the collector and then to use simple models for the pressure-distribution on the front face of the collector. The CFD code was implemented to simulate the flow in the plenum over a range of parameters and to assess the effect of these parameters on the flow distribution. It was, however, restricted to cases where the wind speed is essentially zero.

The present paper extends the study by Gunnewiek *et al.* (1996) (hereinafter called the 'earlier study') to the case where the wind plays an important role. As was the case in the earlier study, the CFD modeling was restricted to the plenum region. The wind was modeled according to the pressure distribution it imposes at the collector face — i.e. the building face — as given by some models taken from the literature and developed from measurements. It had been found in the earlier study that under conditions of low average suction velocity (less than about 0.0125 m/s), buoyancy could induce the highly-undesirable reverse flow, and the present study found that, generally-speaking, the effect of the wind was to raise the minimum suction velocity needed to avoid the reverse-flow phenomenon. Plots of flow distribution under typical wind conditions will be given and conclusions are drawn.

2. DEVELOPMENT OF THE CFD MODEL

Except for special steps required to incorporate the wind, the code was the same one used in the earlier study, which was based on a commercial CFD code (TASCflow). Further details are given by Gunnewiek (1994), who also describes the method of establishing the accuracy and the degree of grid-independence. Thus we give here only a brief summary of the basics of this code, and then add details pertaining to the wind-effect simulation. Fig. 1 shows a schematic of the situation. The transpiration (or suction) was modeled as a continuous phenomenon, rather than a process occurring through discrete holes. Also, only the plenum region (i.e. the $H \times D \times W$ region in Fig. 1) was included in the computational domain.

The plate and the ambient surrounds were modeled by means of a pair of special boundary conditions at the domain's front-face, i.e. the $x = t$ plane in Fig. 1. The first boundary condition was a momentum balance on the air as it passes through the plate, and the second was an energy balance on the plate. In describing the momentum

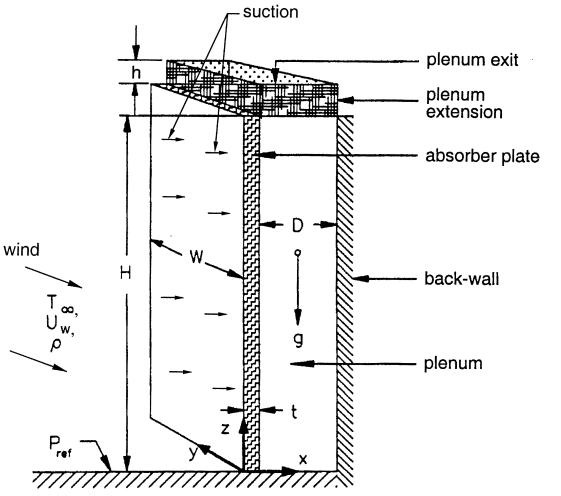

Fig. 1. Dimensional sketch of collector's plenum, showing the co-ordinate system, the approaching wind (which may be oblique to the collector face), and the suction of air perpendicular to the plate.

balance, $P(x, y, z)$ and $u(x, y, z)$ will be used to represent, respectively, the pressure and the x-component velocity at point (x, y, z) of the co-ordinate system shown in Fig. 1. The local pressure drop that the air experiences as it passes through the plate was modeled by the equation

$$P(0, y, z) - P(t, y, z) = K_H \rho [u(t, y, z)]^{3/2} \qquad (1)$$

where K_H is a measure of the plate's hydraulic resistance, and ρ is the air density. (For plates of interest K_H has been found to range between about 750 and about 4000 $(m/s)^{0.5}$. For example, a typical commercial plate with 1% porosity and 1.6 mm diameter holes has K_H equal to 1500 ± 250 $(m/s)^{0.5}$ over a fourfold range (0.02 to 0.08 m/s) in nominal suction velocities.) The pressure at the front face of the plate, i.e. at $x = 0$, was modeled as given by

$$P(0, y, z) = P_{ref} - \rho g z + C_p(y, z)\left[\frac{1}{2}\rho U_w^2\right] \qquad (2)$$

where the first term on the right-hand side is the ambient pressure at ground level, the second term (in which g is the acceleration of gravity and ρ is evaluated far from the plate in the ambient air) is the hydrostatic pressure far away from the plate, and the third term — not included in the earlier study — is the contribution of the wind to the pressure at the front face of the collector plate. In this last term, U_w is the wind speed in the far field, at a height equal to the highest point in the building on which the collector is mounted; here we take this height to be the same as the collector height H (Fig. 1). Also, $C_p(y, z)$ is the local wind

pressure coefficient, the models for which we will discuss later. By combining Eqs. (1) and (2) one obtains a relation between the x-velocity and the pressure at the $x = t$ face, and this relation constitutes the momentum front-face boundary condition.

The second boundary condition results from an energy balance on the front-face, which reduces to

$$T(t, y, z) = T_\infty + \frac{(\alpha G)_n}{\rho c_p u(t, y, z) + U_o} \tag{3}$$

where $T(t, y, z)$ is the temperature of the air as it leaves the plate at the $x = t$ face, T_∞ is the ambient air temperature far from the plate, $(\alpha G)_n$ is the net absorbed solar energy at the plate, c_p is the specific heat of air, and U_o is the ratio h_r to ϵ_{HX}, where h_r is the radiant heat loss coefficient from the plate to the ambient surrounds temperature and ϵ_{HX} is the plate heat exchange effectiveness (Kutscher, 1994; Van Decker *et al.*, 2001).

The fan downstream of the plenum is assumed to produce either a prescribed flow Q m^3/s or a prescribed pressure P_{out} that is uniform across its entrance plane. It is assumed to be connected to the plenum by means of a straight, slip-walled duct extending a sufficiently large distance from the plenum that the plenum flow no longer depends on this distance. The back-wall plane at $x = D + t$ and the floor $z = 0$ were assumed to be adiabatic. The flow in the plenum was assumed to be turbulent, and the k–ϵ turbulence model was used to model the turbulence.[1]

The computational grid, which divides the domain into small but finite volumes (or elements), was constructed in such a way that the elements were smaller (by about one-tenth) in the region near the absorber plate as compared with those near the back wall of the plenum. A grid-refinement study showed that a grid with 20 element divisions in the x-direction and 100 element divisions in the z-direction was sufficiently fine to give answers of reasonable accuracy[2] (within about 1%) and did not require an inordinate computational effort. So this division was used in all the 2D simulations reported here. In the 3D simulations, which allowed for variation in the y-direction, similar element divisions were used in the x- and z-directions as for the 2D studies, but in addition there were 24 divisions in the y-direction for the frontal wind case and 45 divisions in the y-direction for the quartering wind case, these cases being defined in what follows.

[1]As justified in the earlier study, the turbulence assumption was based on the Reynolds number range and classical smooth pipe observations. Also, the jetting action of the suction holes was expected to induce turbulence.

[2]Described in the previous study, the grid-refinement study involved solving the problem using three grids of increasingly large values of the number of nodal points N, and then extrapolating the solution to $N = \infty$, which was then assumed to be the true solution. The error was then estimated as the difference between this true solution and the solution obtained with the grid actually used.

3. MODELS FOR THE WIND PRESSURE COEFFICIENT, $C_p(Y, Z)$

The wind effects on buildings depend on the orientation of the building with respect to the wind and the building shape. When the wind is incident on the building face opposite to the one on which the collector is mounted, the collector face will be almost entirely in a separated region, and under this condition the C_p tends to be uniform, and since a uniform distribution produces no effect on the collector velocity distribution per se, this situation tends to be less interesting than other orientations. The more interesting cases arise when the wind is frontal on the collector or when the wind is coming a-glance on the collector, as is illustrated by the case of a 'quartering wind' where the wind is incident at 45 degrees to the collector surface.

The distribution of the local wind pressure coefficient $C_p(y, z)$ on a building has been the subject of several investigations and recent findings are reviewed by ASHRAE (1997). ASHRAE (1997) recommends that for any particular building and local topography, wind tunnel studies be performed to obtain the pressure distribution, and they provide guidelines for carrying out these wind tunnel studies. The wind-pressure coefficients used in the present studies were based partly on the studies of Hunt (1982), Davenport and Hui (1982), and Holmes (1986) and partly on supporting wind tunnel studies conducted in accordance with the ASHRAE guidelines, using the flexible-walled wind tunnel at the University of Waterloo (Brundrett and Kankainen, 1991). The distributions used assume a smooth terrain in front of the building, and the building is assumed to be immersed in an atmospheric boundary layer, so that the wind speed increases with distance up from the ground, according to a standard equation (see, for example, ASHRAE, 1997). The reference location for the wind speed is the wind speed at the top of the building.

As the wind approaches the building, there is a

conversion from dynamic pressure to static pressure, in accordance with Bernoulli's theorem. On the windward face of the building there will generally be a stagnation point, where the pressure coefficient is maximum because there the air has been brought to a complete standstill; however, because of the vertical variation in wind speed, the value of the pressure coefficient at the stagnation point will be less than the unity value normally observed on bluff bodies in the absence of ground effects. Because the air has to accelerate to get around the building, the velocities near the edges of the windward face tend to be higher than the far field values, and so there is a reduced pressure near the edges.

In the present study, simulations were conducted for three combinations of building shape and orientation. The first is a frontal wind on a very long building with W/H large, which results in the 2D situation in which there is no dependence on y (except for a small region at the two ends of the collector). Fig. 2 illustrates the relevant pressure coefficient distribution applying in this case, the one used in the simulations reported here. In the figure, $Z^* = z/H$ represents the dimensionless height up the building face from ground level. The point of maximum pressure occurs at $Z^* \approx 0.82$, and the pressure coefficient there is 0.6. The acceleration of the flow to go over the top of the building causes the pressure coefficient to reduce to 0.28 at the very top. Fig. 3a and b, which are based on the experimental work of Hunt (1982), Davenport and Hui (1982), and Holmes (1986), show typical contours of the wind pressure coefficient on a cubical building with a frontal and quartering wind, respectively. In both cases there is a maximum pressure point near the top, and a rapid falling off of pressure as one approaches the roof. In the case of the quartering wind, the maximum pressure point occurs on the windward edge. Figs. 2 and 3, together with an assumed wind speed at the building top of 5 m/s, were used in the simulations reported below.

The choice of 5 m/s for the wind speed was based on the observation that for most urban locations, this wind speed will be exceeded only about 15% of the time. For example in a study of convective heat losses from solar collectors, Test *et al.* (1981) observed an average wind speed (over a 4-h period) greater than 5 m/s only in one of seven runs. In a similar study Sharples and Charlesworth (1998) found in their experiments that (hourly-averaged) wind speeds of 1, 3, and 5 m/s were representative; presumably of low, medium, and high winds. So we concluded that 5 m/s is suitably representative of a high wind, and since high winds are more problematic for the UTC, we chose this setting for the simulations.

4. RESULTS

4.1. Results for the 2D case ($W/H \gg 1$)

As was the case in the previous study, simulations were carried out under a range of settings of

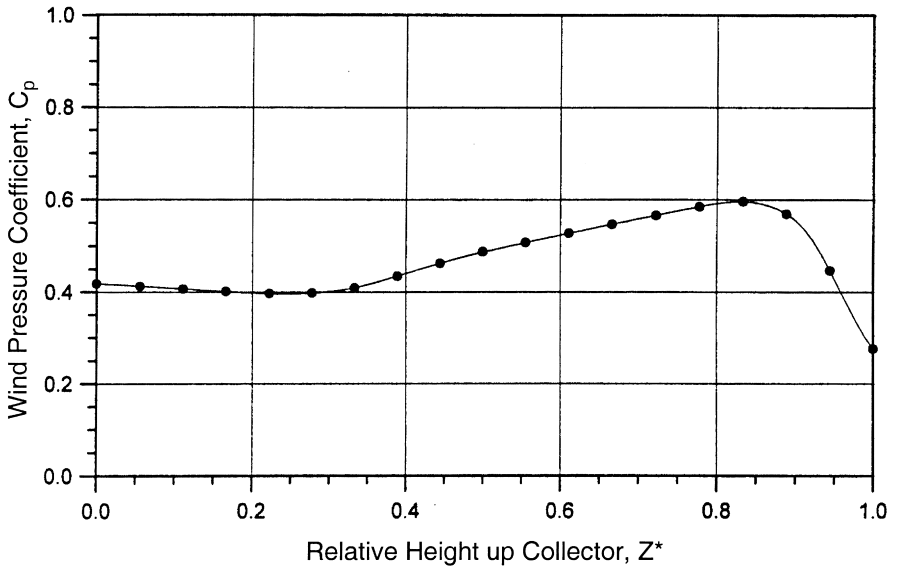

Fig. 2. Plot of model for the $C_p(y, z)$ distribution used to represent the case of the collector facing directly into the wind and mounted on the long face of a very long building.

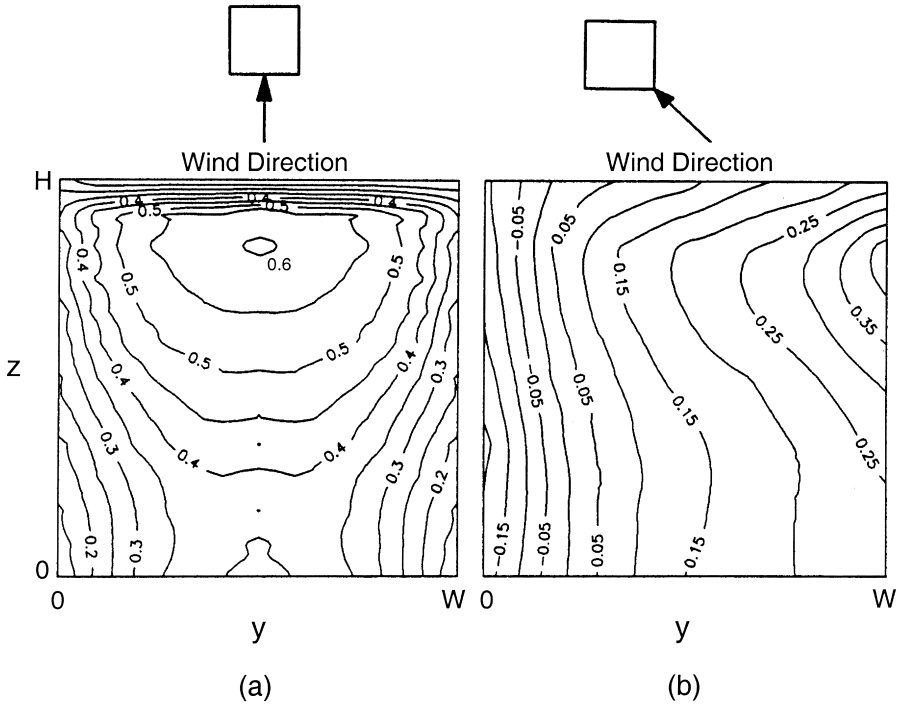

Fig. 3. Contour lines of model for the $C_p(y, z)$ distribution used for the collector mounted on a cubical building and (a) facing directly into the wind or (b) facing a quartering wind. The iso-C_p lines are at 0.05 steps in C_p.

the important parameters. Firstly, a 'typical configuration' was run, this being defined as the following combination of settings for the parameters: $H = 4.5$ m, $(\alpha G)_n = 650$ W/m^2, $U_o = 5$ W/m^2 K, $H/D = 30$, $K_H = 2250$ m$^{0.5}$ s$^{-0.5}$, and average suction velocity, $u_{ave} = Q/(WH) = 0.02$ m/s. Then each parameter was varied in turn and runs made. Except for the setting of u_{ave}, a similar procedure was followed in the present study. Fig. 4 shows the results for the case in which u_{ave} was varied over three different settings. The quantity plotted is the suction velocity profile up the plate (normalized by division by u_{ave}), which is the chief hydrodynamic quantity of interest. Also plotted in this figure — as a dashed line — are the ('no-wind') results obtained in the earlier study at the midline value of u_{ave}, namely $u_{ave} = 0.02$ m/s. The influence of the wind is seen to be quite profound, particularly at low values of u_{ave}. The sudden falling off of the suction velocity at $Z^* > 0.8$ is to be particularly observed, and it is clearly a result of the falling off of C_p in this Z^* range that was observed in Fig. 2. For u_{ave} as high as 0.08 m/s, the effect has been overpowered by the corresponding increase in the pressure drop across the plate.

One of the important factors one looks for in the velocity profile is the phenomenon of reverse flow (or 'outflow'): this happens when the flow over some part of the plate is out rather than in, and it should be avoided under all but the most extreme operating conditions, because not only is the heat absorbed over that part wasted, but some heat already collected at another part of the plate is being discarded. It can be seen that reverse flow at the very top of the plate is almost achieved at $u_{ave} = 0.0164$, and indeed for average suction rates only slightly less than that setting, reverse flow was observed. The minimum flow rate for no wind conditions had previously been reported to be 0.0125 m/s, and now, in light of the present findings this number has to be raised to 0.0164 m/s for a long building in a frontal wind of 5 m/s. Fig. 5 shows similar plots to those shown in Fig. 4, except different parameters were varied. These results show that the u_{ave} was the variable that had the strongest effect, but that K_H and H/D were also very important, and that values of K_H less than 750 $(\text{m/s})^{0.5}$ and of H/D greater than 50 should be avoided, as under these conditions the velocity at the top of the collector approaches zero. Details are given by Gunnewiek (1994).

It was shown in the earlier study that, provided there is no reverse flow, quite a large variation in the velocity profile can be tolerated without unduly affecting the collector efficiency, and the same result was found for the cases with the 5 m/s wind (Gunnewiek, 1994). Thus, the main

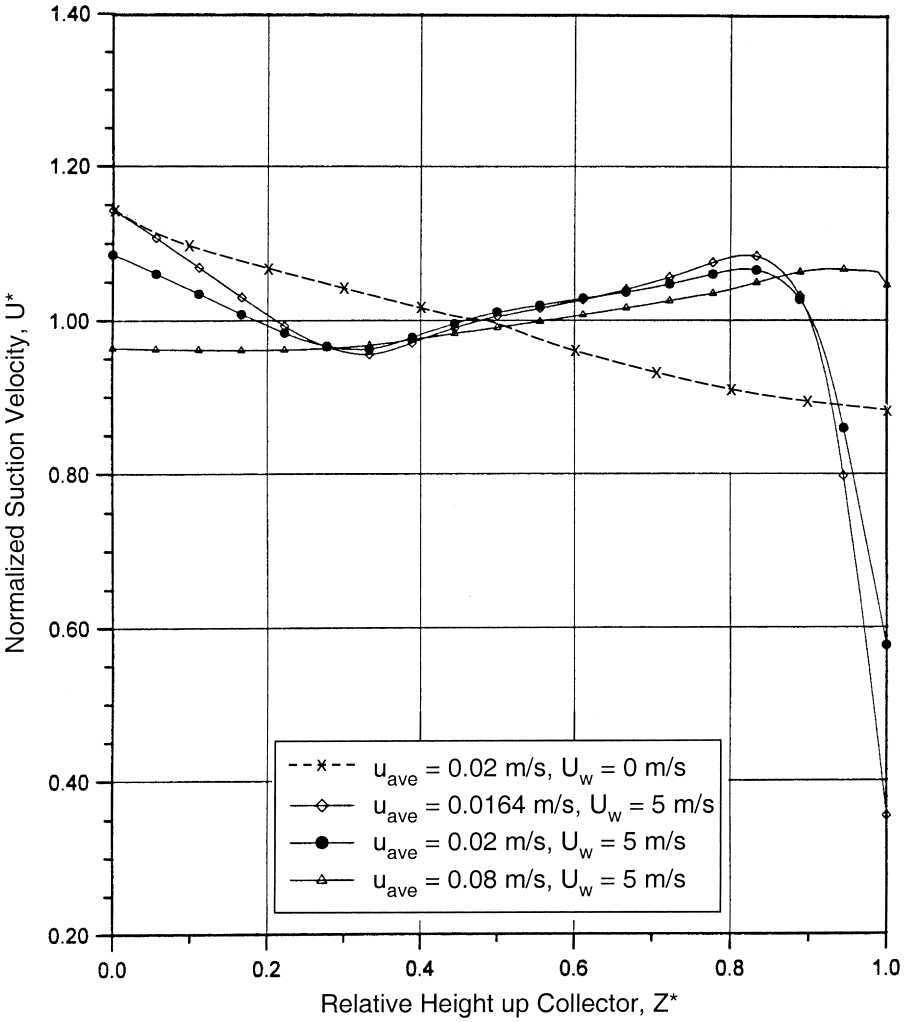

Fig. 4. Normalized suction velocity profiles for the $C_p(y, z)$ model shown in Fig. 2, at three settings of u_{ave} and with the other parameters at their 'typical configuration' settings. All curves are for a wind of 5 m/s except for the dashed line, which is for no wind with $u_{ave} = 0.02$ m/s.

cause for concern is flow reversal itself. The earlier study also gave a physical explanation that accounted for the shape of the observed velocity profiles. The flow was pictured as the superposition of two flows: a buoyant flow driven by the temperature differences developed by the absorbed solar energy, and a forced flow developed by the fan. If each were to act in the absence of the other, their flows would develop quite different profiles: buoyant flows have smaller suction velocities at the top and forced flows have smaller suction velocities at the bottom. The observed profile depends on which flow mechanism is dominating at the particular set of parameter settings. In light of this, one might ask what flow profile the wind would develop if it were acting alone. This may be inferred from the pressure coefficient profile, such as is shown in Fig. 2, which would tend to produce less flow at both bottom and top with a maximum in between.

In broad terms the observed profiles under wind conditions can be explained as a superposition of now three flows, none of which dominates except at extreme parameter settings. The critical appearance of reverse flow at the top will be reinforced when both wind and buoyant effects are dominant, because both tend to produce less flow at the top. This is exemplified in Fig. 4 at $u_{ave} = 0.02$ m/s, where the buoyancy-dominated no-wind situation is reinforced by the wind — both types of flow tending to produce lower flow at the top.

4.2. Results for 3D case: the cubical building

Figs. 6 and 7 show contour lines of normalized velocity for the cases of the frontal and quartering wind on the cubical building, respectively. These

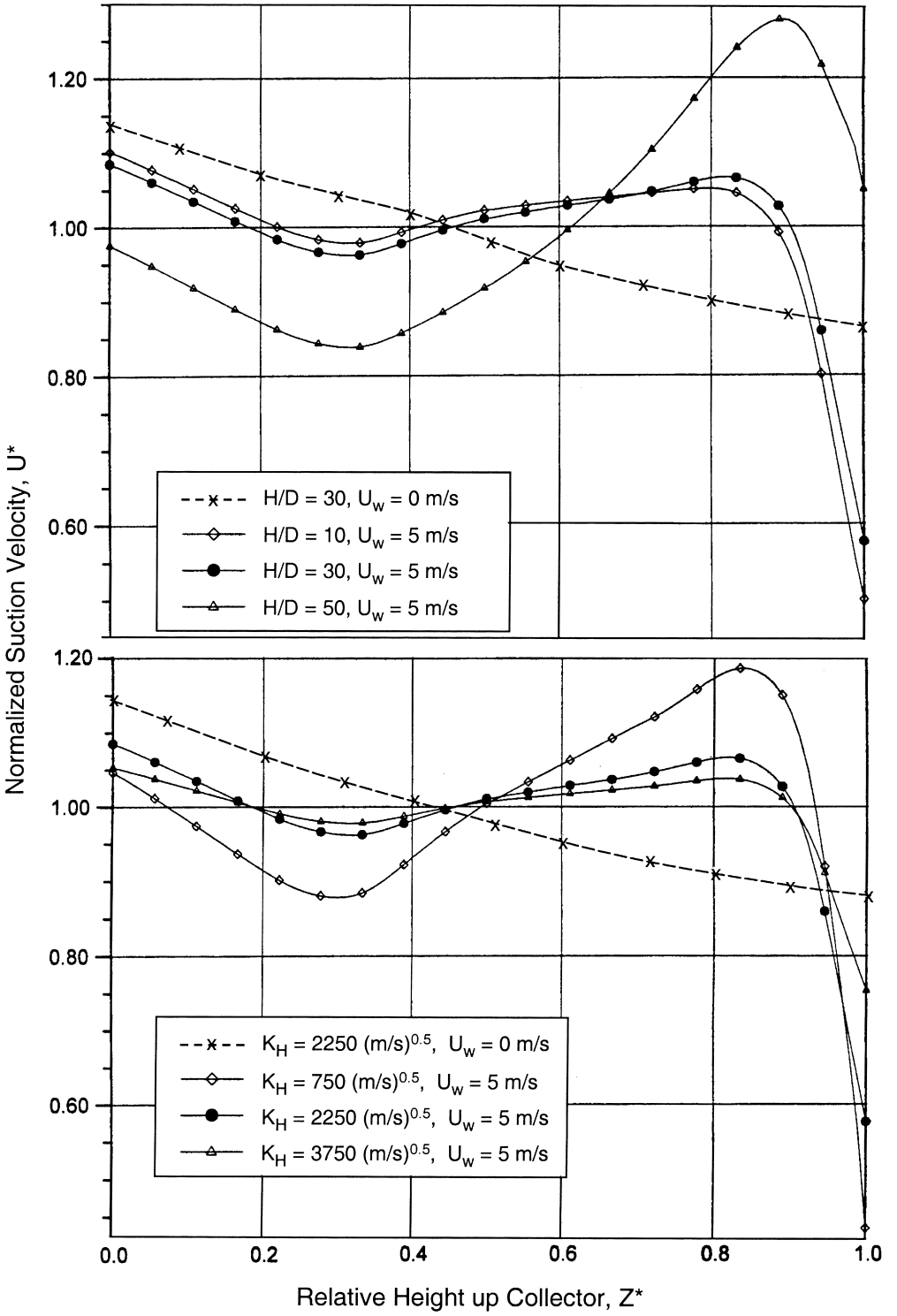

Fig. 5. Normalized suction velocity profiles for the $C_p(y, z)$ model shown in Fig. 2, at three settings of K_H and three settings of H/D and with the other parameters held at their 'typical configuration' settings. All curves are for a wind of 5 m/s except for the dashed line, which is for no wind.

lines follow somewhat the iso-C_p contours shown in Fig. 2, indicating that the wind is having an important effect. As for the 2D case, it was found that the effect of the non-uniform flow had only a very minor effect on the average collector efficiency. However it was found that the minimum u_{ave} to avoid reverse flow was increased in the 3D case, going to 0.0263 m/s for the 3D frontal wind

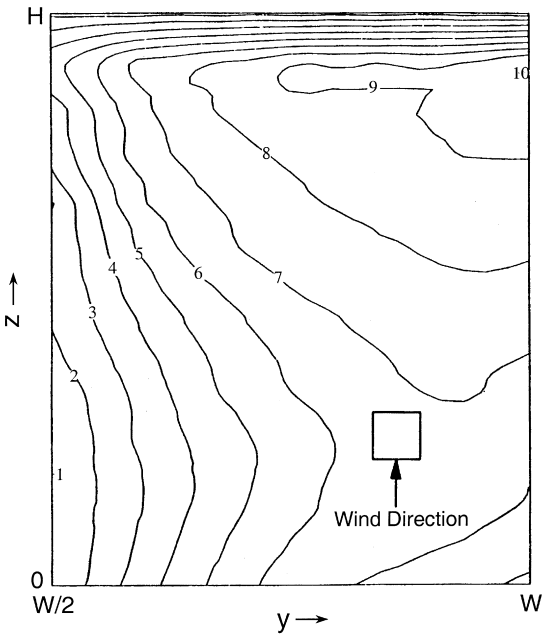

Fig. 6. Normalized suction velocity contours for the situation shown in Fig. 3a, at $u_{ave} = 0.02$ m/s and wind speed $U_w = 5$ m/s, and the typical configuration settings for all the other parameters. Only the region having $W < y < W/2$ is shown, the contours are symmetric about the plane $y = W/2$. U^* ranges from 0.794 on contour line 1 to 1.16 on contour line 10, and the contour lines are shown for equal increments U^* between these two extremes.

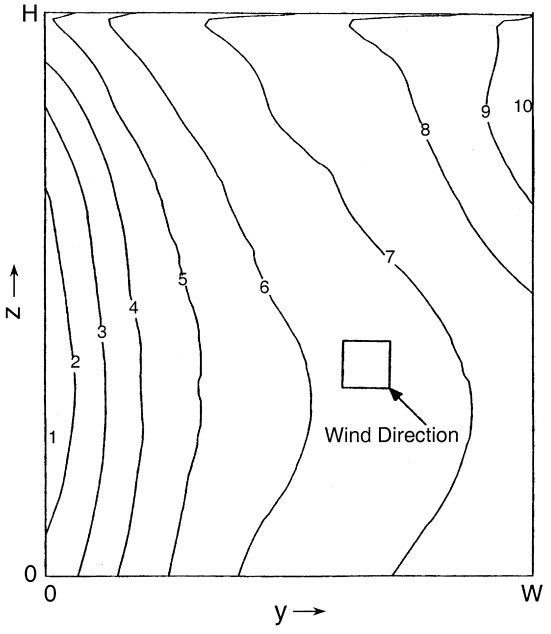

Fig. 7. Normalized suction velocity contours for the situation shown in Fig. 3b, at $u_{ave} = 0.02$ m/s and wind speed $U_w = 5$ m/s, and the typical configuration settings for all the other parameters. U^* ranges from 0.81 on contour line 1 to 1.15 on contour line 10, and the contour lines are shown for equal increments U^* between these two extremes.

case and up to 0.039 m/s in the 3D quartering wind case. Further details, including plate temperature distributions, are given by Gunnewiek (1994).

5. CONCLUDING REMARKS

The wind has a pronounced effect on the velocity distribution, but not so large an effect as to negate operating the collector under windy conditions. The main effect is to raise the suction rate needed to avoid reverse flow, from about 0.0125 m/s under typical operating conditions, to about 0.017 m/s for long buildings with the collector facing into the wind, to about 0.026 m/s for cubical buildings with the collector facing into the wind, and to about 0.039 m/s for a cubical building with the wind incident on the collector at 45°. These numbers are for a wind speed at building height of 5 m/s, which is a higher than average wind speed for most locations.

Often one wants a design suction rate below these minimum values but above the value permitted for no wind. In this case one may look to adopting one of several possible strategies. Firstly, since the effect of the wind on the velocity distribution is almost completely localized to a region just below the roof-line, an excellent strategy would seem to be to leave this area (which, in height, is about one-tenth of the building height) free of solar collector. Another strategy could be to monitor the wind and to increase the flow rate of air under conditions of high wind. Finally, one could just accept the fact that there will be some reverse flow under high wind conditions. To evaluate this strategy one would need to know more about the reverse flow — for example the area it covers — than was covered in this paper.

NOMENCLATURE

A	collector area, $= WH$, m^2
$C_p(y, z)$	pressure coefficient at point (0, y, z) on face of building/collector, dimensionless
c_p	specific heat of air, J/kg K
D	plenum depth, Fig. 1, m
G	solar irradiance incident on collector, W/m^2
g	acceleration of gravity, m/s^2
H	collector height, Fig. 1, m
h_r	radiative heat transfer coefficient from plate to ambient surrounds, W/m^2 K
K_H	plate's hydraulic impedance, $m^{1/2}\ s^{-1/2}$
$P(x, y, z)$	static pressure at co-ordinate (x, y, z), Pa
P_{ref}	atmospheric pressure at ground, Pa
Q	volumetric flow rate at which air is drawn over entire collector face, m^3/s

q_b	heat flow at the back of the collector plate that occurs by convection to the air in the plenum, W
$T(x, y, z)$	air temperature at co-ordinate (x, y, z), K
T_∞	ambient air temperature, = inlet temperature to solar collector, K
t	absorber plate thickness, Fig. 1, m
U_o	an apparent overall heat transfer coefficient, $= h_r/\epsilon_{HX}$, W/m^2 K
U_w	wind speed, m/s
U^*	normalized suction velocity, $= u(t, y, z)/u_{ave}$
$u(x, y, z)$	x-component of air velocity at co-ordinate (x, y, z), m/s
u_{ave}	average suction velocity, $= Q/A$, m/s
W	width of collector, Fig. 1, m
(x, y, z)	co-ordinate of a general point, according to the co-ordinate system of Fig. 1
Z^*	z/H

Greek symbols

α	plate solar absorptivity, dimensionless
$(\alpha G)_n$	$\alpha G - q_b/A$, W/m^2
ϵ_{HX}	plate's heat exchange effectiveness, dimensionless
ρ	density of air, kg/m^3

Acknowledgements—Financial support for this work was provided by the Natural Sciences and Engineering Research Council (Canada) under a Strategic Grant. We also thank AEA Technology Engineering Software, Waterloo, Ontario, Canada for assistance in the use of their code.

REFERENCES

Arulanandam S. J., Hollands K. G. T. and Brundrett E. (1999) A CFD heat transfer analysis of the transpired solar collector under no-wind conditions. *Solar Energy* **67**(1–3), 93–100.

ASHRAE (1997) Airflow around buildings. In *1997 ASHRAE Handbook of Fundamentals*, pp. 1–18, American Society of Heating, Refrigeration and Air-Conditioning Engineers, Atlanta, GA, USA, Chapter 15.

Brundrett E. and Kankainen P. (1991) The construction and commissioning of a flexible walled wind tunnel. *Can. Aeronaut. Space J.* **37**(3), 108–119.

Carpenter, S. C. and Kokko, J. P. (1991) Performance of solar preheating ventilation systems. In *Proceedings Annual Conference of Solar Energy Society of Canada*, June 21–26, Toronto, Solar Energy Society of Canada Inc., Ottawa, pp. 261–265.

Davenport A. G. and Hui H. Y. L. (1982). *External and Internal Wind Pressures on Cladding of Buildings, Report of the Boundary Layer Wind Tunnel Laboratory*, University of Western Ontario, London, Ontario, Canada, Report no. BLWT-820133.

Dymond C. and Kutscher C. (1997) Development of a flow distribution and design model for transpired solar collectors. *Solar Energy* **60**, 291–300.

Ferziger J. H. and Peric M. (1997). *Computational Methods for Fluid Dynamics*, Springer, New York.

Gunnewiek L. H. (1994). *An Investigation of the Flow Distribution through Unglazed Transpired-plate Solar Air Heaters*, Department of Mechanical Engineering, University of Waterloo, Waterloo, Ontario, Canada, M.A.Sc. Thesis.

Gunnewiek L. H., Brundrett E. and Hollands K. G. T. (1996) Flow distribution in unglazed transpired-plate solar air heaters of large area. *Solar Energy* **58**, 227–237.

Hollick J. C. and Peter R. W. (1990) United States Patent No. 4,934,338.

Holmes J. D. (1986). *Wind Tunnel Loads on Low Rise Buildings: the Structural and Environmental Effects of Wind on Buildings and Structures*, Faculty of Engineering, Monash University, Melbourne, Australia.

Hunt A. (1982) Wind-tunnel measurements of surface pressures on cubic building models at several scale. *J. Wind Eng. Ind. Aerodyn.* **10**, 137–163.

Kutscher C. F. (1994) Heat exchanger effectiveness and pressure drop for air flow through perforated plates with and without crosswind. *J. Heat Transfer* **116**, 391–399.

Kutscher C. F., Christensen C. and Barker G. (1991) Unglazed transpired solar collectors: an analytic model and test results. In Proceedings of ISES Solar World Congress 1991, Vol. 2, pp. 1245–1250, Elsevier Science, Part 1.

Kutscher C. F., Christensen C. and Barker G. (1993) Unglazed transpired solar collectors: heat loss theory. *ASME J. Solar Eng.* **115**(3), 182–188.

Sharples S. and Charlesworth P. S. (1998) Full-scale measurements of wind-induced convective heat transfer from a roof-mounted flat plate collector. *Solar Energy* **62**, 69–77.

Test L. F., Lessmann R. and Johary A. (1981) Heat transfer during a wind flow over rectangular bodies in the natural environment. *J. Heat Transfer* **103**, 262–267.

Van Decker G. W. E., Hollands K. G. T. and Brunger A. P. (2001) Heat-exchange relations for unglazed transpired solar collectors with circular holes on a square or triangular pitch. *Solar Energy* **71**, 33–45.